

## Supporting Information for

# **Super-2D Metal Organic Frameworks with Vertical Layer Skeletons and Good Adsorption Performances**

Pan Yang and Youfu Wang\*

School of Chemistry and Chemical Engineering,  
Frontiers Science Center for Transformative Molecules,  
Shanghai Jiao Tong University.

800 Dongchuan Road, Shanghai 200240, P. R. China.

E-mail: wyfown@sjtu.edu.cn

## Table of Contents

<b>1. General Information</b> .....	S3
<b>2. Experimental Section</b> .....	S4
<b>Scheme S1.</b> The synthetic route of the pentiptycene catechol ligand, <b>L</b> . ....	S4
<b>Fig. S1</b> The PXRD plots of the super-2D MOFs. ....	S6
<b>Fig. S2</b> The experimental and simulated XRD patterns of super-2D MOFs with star-shaped structure. ....	S7
<b>Fig. S3</b> The experimental and simulated XRD patterns of super-2D MOFs with rhombic-shaped network. ....	S8
<b>Fig. S4</b> The TEM images of (A, B) MOF(Cu) and (C, D) MOF(Zn). ....	S9
<b>Fig. S5</b> The full XPS spectrum of the MOF(Ni). ....	S10
<b>Fig. S6</b> The XPS plots of each elements within the MOF(Ni). ....	S11
<b>Fig. S7</b> The FT-IR spectra of <b>L</b> and MOF(Ni). ....	S12
<b>Fig. S8</b> The UV-Vis-NIR and UPS spectra of MOF(Ni). ....	S13
<b>Fig. S9</b> The CV curves and band energy of <b>L</b> and MOF(Ni). ....	S14
<b>Fig. S10</b> The TGA plots of <b>L</b> and MOF(Ni) under oxygen. ....	S15
<b>Fig. S11</b> The standard curve of I <sub>2</sub> in cyclohexane. ....	S16
<b>Fig. S12</b> The UV-Vis curves of I <sub>2</sub> in supernatant after adsorption with MOF(Ni) for different times. ....	S17
<b>Fig. S13</b> The standard curves of PAHs in CH <sub>3</sub> CN. ....	S18
<b>Supporting References</b> .....	S20

## 1. General Information

**XRD:** The PXRD patterns of MOFs were collected on a Bruker D8 Advance diffractometer using Cu K $\alpha$  radiation ( $\lambda = 1.5418 \text{ \AA}$ ) or synchrotron radiation in Shanghai Synchrotron Radiation Facility (SSRF).

**HRTEM:** The morphologies, sizes and elemental mappings of the super-2D MOFs were estimated by high resolution transmission electron microscopy (HRTEM) on Talos F200X (USA).

**XPS:** The XPS of MOFs were performed on an Ultra DLD system, the C 1s value was set at 284.8 eV for charge corrections.

**FT-IR:** Fourier transform infrared (FT-IR) spectra were recorded on a Bruker Tensor 27 FT-IR using ATR measurements for solids as neat samples.

**BET:** The nitrogen sorption isotherms were measured on a BELSORP adsorption analyzer at liquid nitrogen temperature, and the surface area was calculated based on the adsorption curve according to the Brunauer-Emmett-Teller (BET) theory.

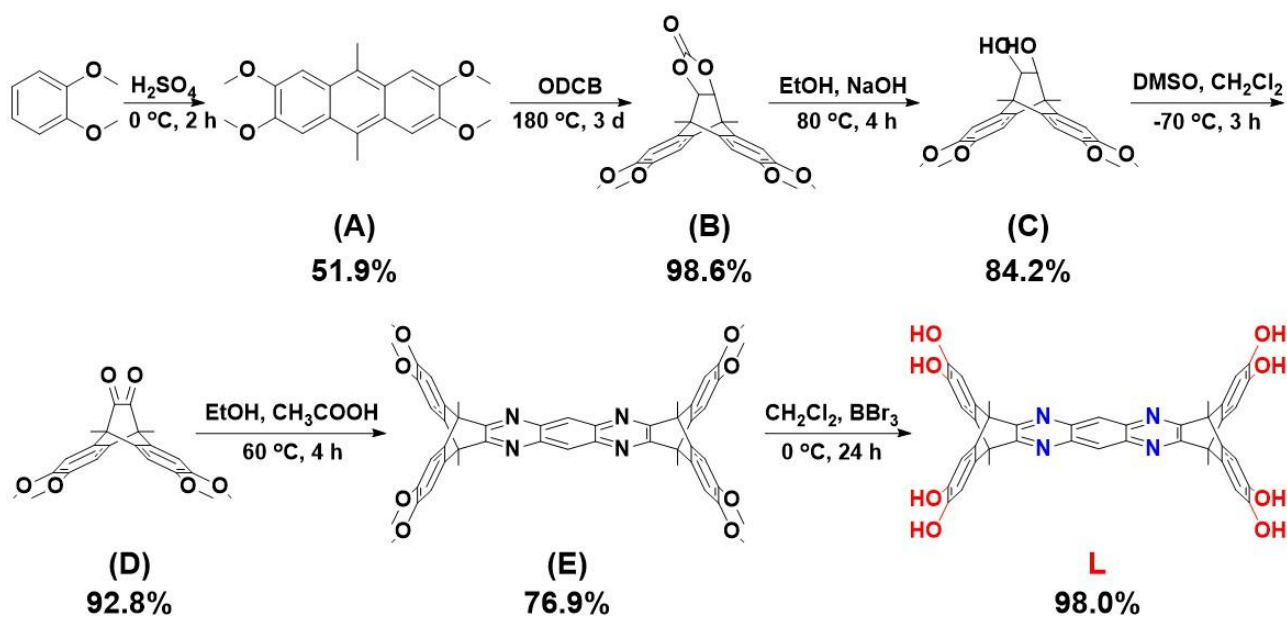
**UV-Vis-NIR:** Ultraviolet-Visible (UV-Vis) spectra were recorded on a Lambda 950 UV-Vis-NIR spectrophotometer by using a 10 mm optical-path quartz cell at room temperature.

**CV:** Cyclic voltammetry (CV) was performed on a CHI 650E electrochemical analyzer in anhydrous CH<sub>3</sub>CN.

**TGA:** Thermal gravimetric analysis (TGA) was performed using a TG 209 F1 Libra thermos gravimetric analyzer in flowing air atmosphere.

**UV-Vis:** Ultraviolet-visible (UV-Vis) absorption spectrum was processed by Thermo Electron-EV300 UV-Vis spectrophotometer.

## 2. Experimental Section



**Scheme S1** The synthetic route of the pentaipyrene catechol ligand, **L**.

### The synthesis of super-2D MOFs with different metals (Ni Cu Zn)

The azaacene bridged pentaipyrene catechol ligand, **L**, was synthesized following the synthetic route in **Scheme S1** and detailed in our previous report.<sup>[1]</sup> **L** (85.7 mg, 0.12 mmol) was dispersed in tetrahydrofuran (15 mL) in a glass vial. Then aqueous solution (5 mL) of  $\text{M}(\text{OAc})_2 \cdot x\text{H}_2\text{O}$  (0.24 mmol,  $\text{M} = \text{Ni}, \text{Cu}, \text{Zn}$ ) was added.<sup>[2]</sup> The vial was capped, sonicated for 15 minutes and then placed in  $85\text{ }^\circ\text{C}$  oven for 72 hours. The reactant was filtered and washed with DMF, water and acetone several times and then dried under vacuum at room temperature overnight to obtain the black red super-2D MOF powders (fields > 89%).

### **The Iodine Adsorption of MOF(Ni)**

The iodine adsorbing capability of the MOF(Ni) was run in cyclohexane since there is no dissociative charge transfer between iodine and cyclohexane.<sup>[3]</sup>

The MOF(Ni) powder (10 mg) was added to the iodine solution of cyclohexane (1 mg/mL, 10 mL) in a glass vial. The sealed vial was shaken by hand to mix them and stood on the table. Then a small aliquot of solution (0.5 mL) was taken out at different times and fresh cyclohexane (0.5 mL) was added to the vial. The extracted solutions were filtered to test UV-Vis spectra.

### **The PAHs Adsorption of MOF(Ni)**

The PAHs adsorbing capability of the MOF(Ni) was assessed in CH<sub>3</sub>CN. The MOF(Ni) (10 mg) was added to the PAH solutions of CH<sub>3</sub>CN (1 mg/mL, 10 mL) in a glass vial. The sealed vials were shaken by hand to mix them and stood on the table. Then a small aliquot of solution (0.5 mL) was taken out at 12 and 24 hours and filtered to test UV-Vis spectrum.

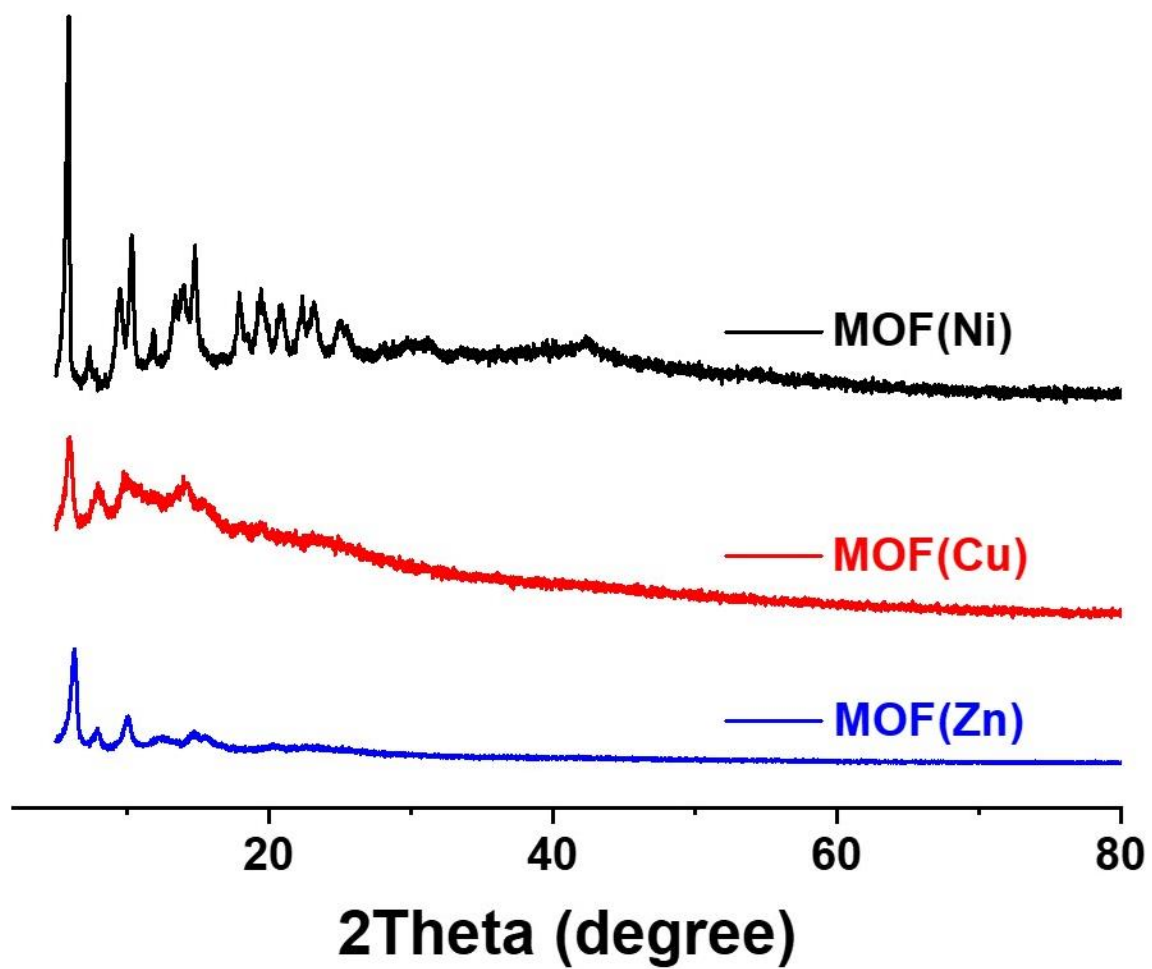


**Fig. S1** The PXRD plots of the super-2D MOFs.

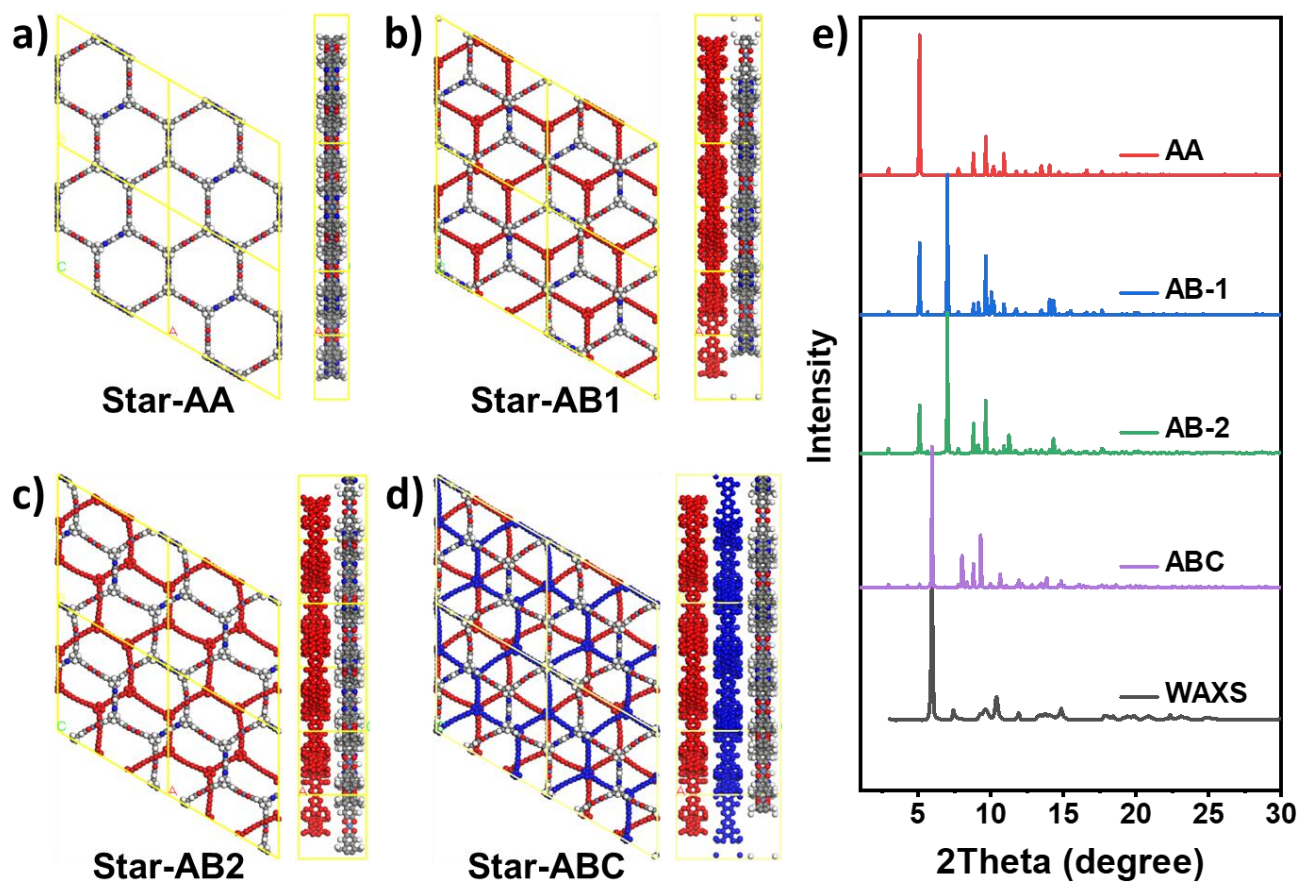


**Fig. S2** The experimental and simulated XRD patterns of super-2D MOFs with star-shaped structure.

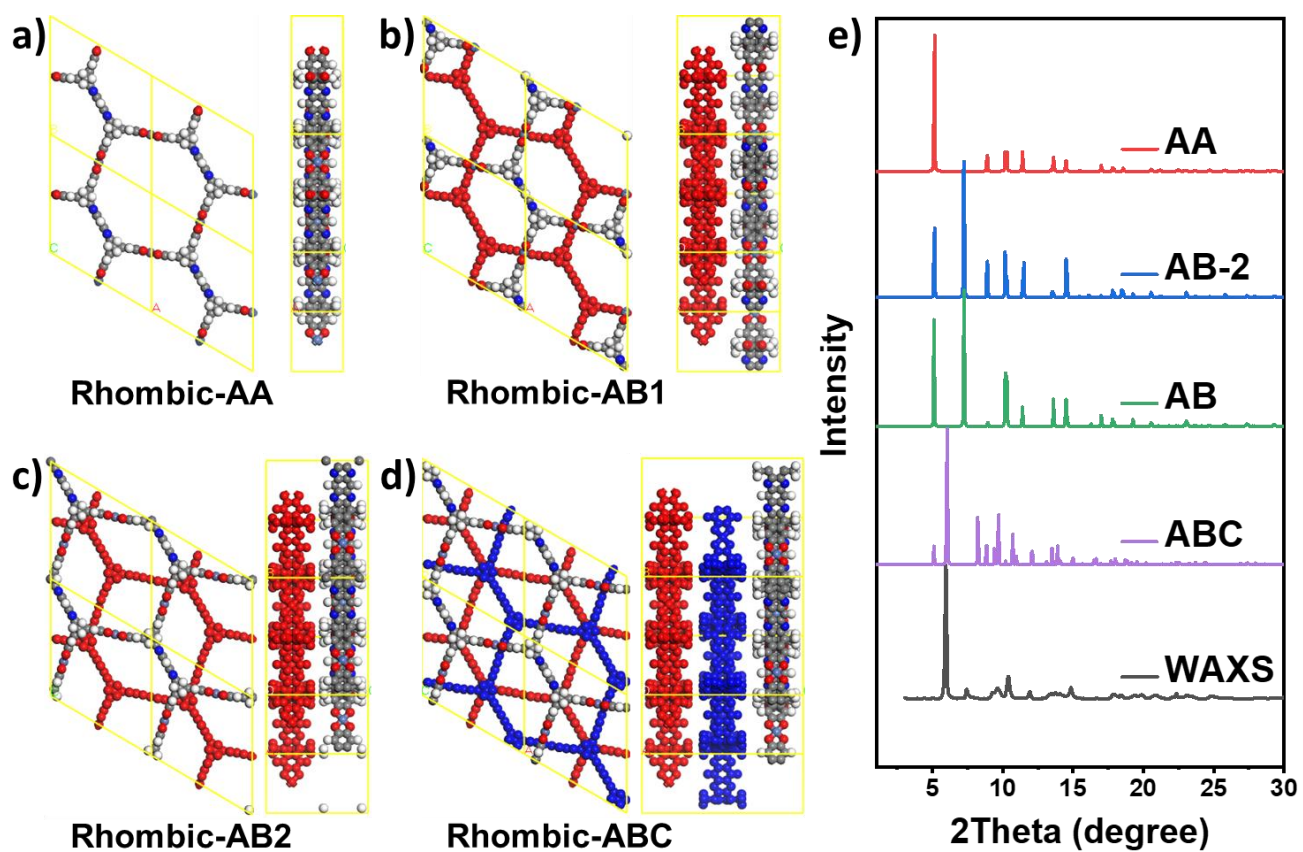


**Fig. S3** The experimental and simulated XRD patterns of super-2D MOFs with rhombic-shaped network.



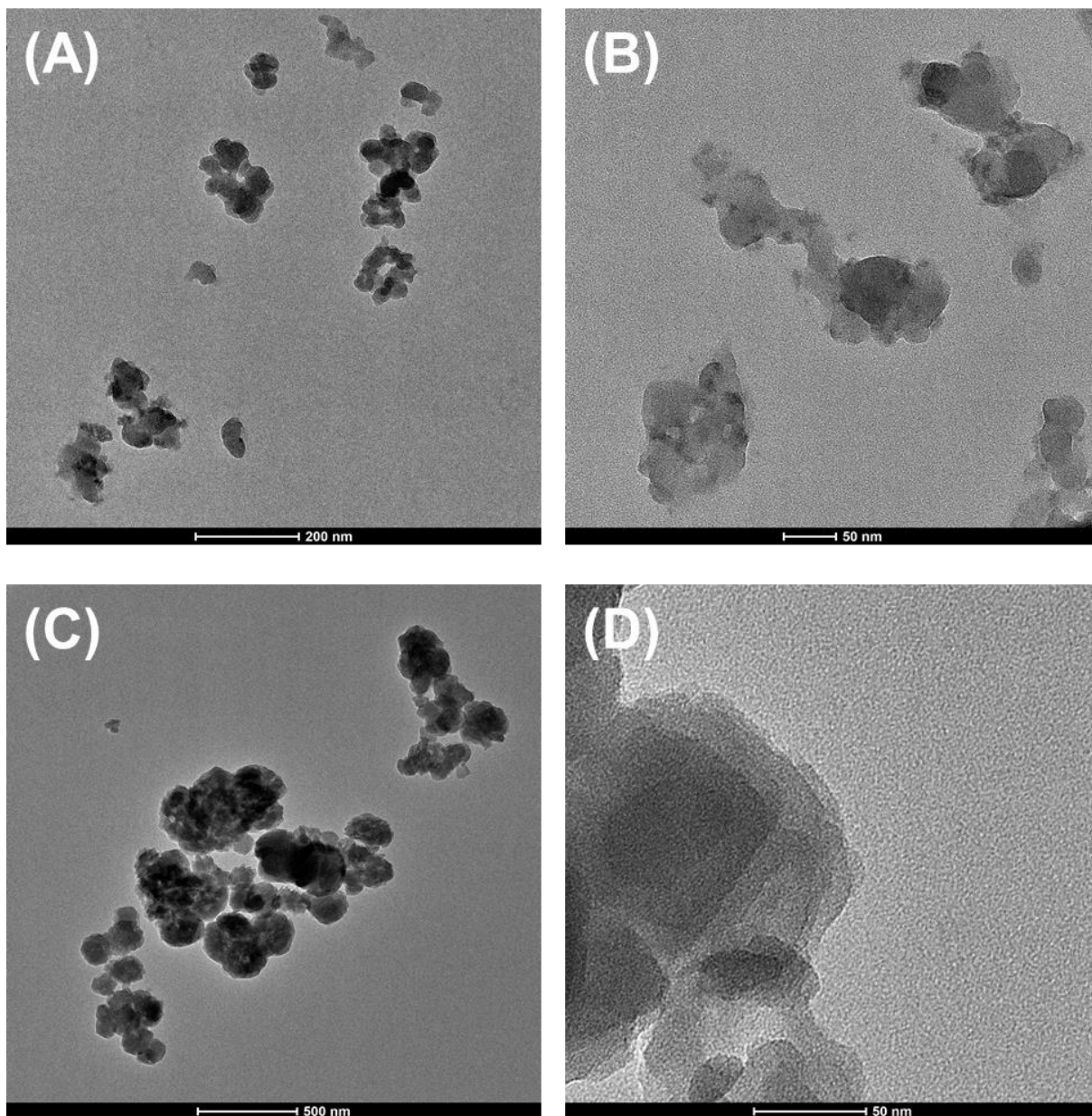


**Fig. S4** The TEM images of (A, B) MOF(Cu) and (C, D) MOF(Zn).

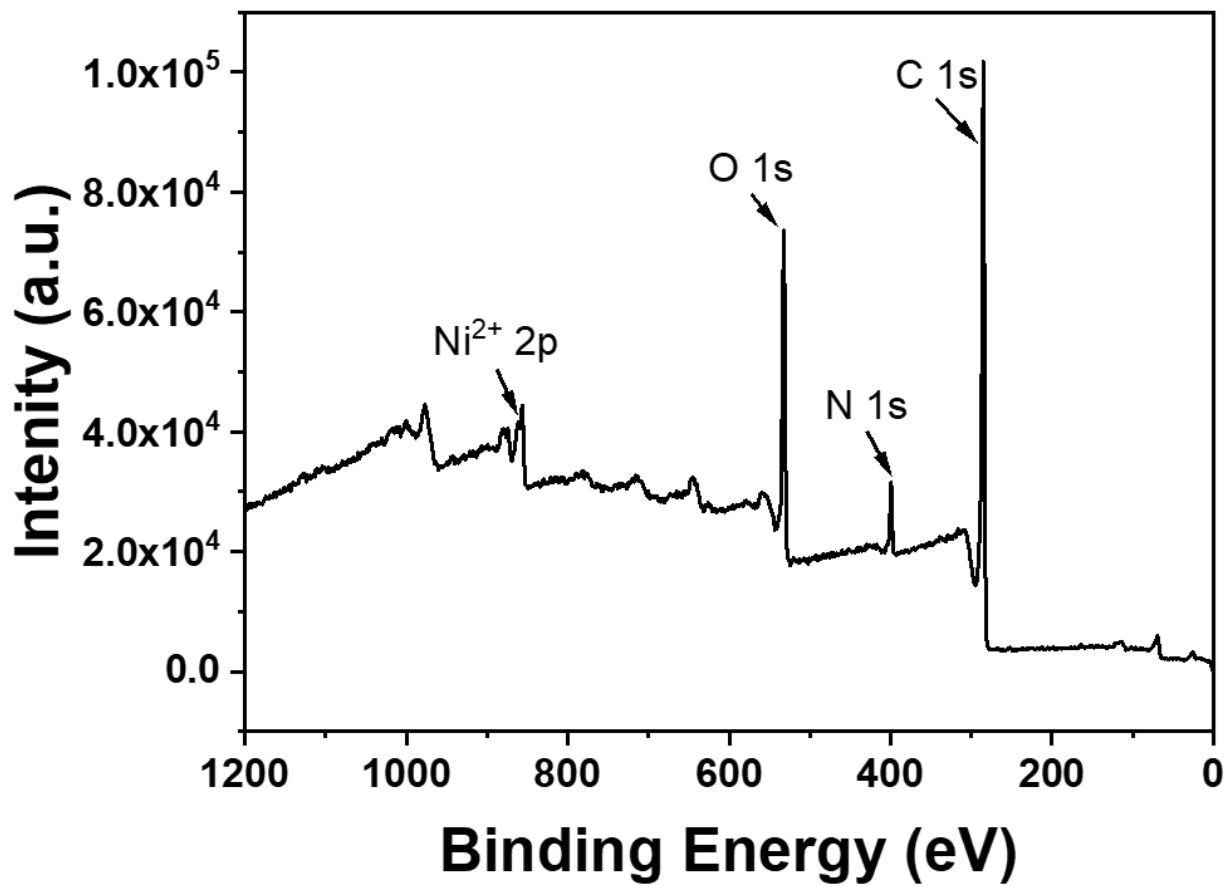


**Fig. S5** The full XPS spectrum of the MOF(Ni).

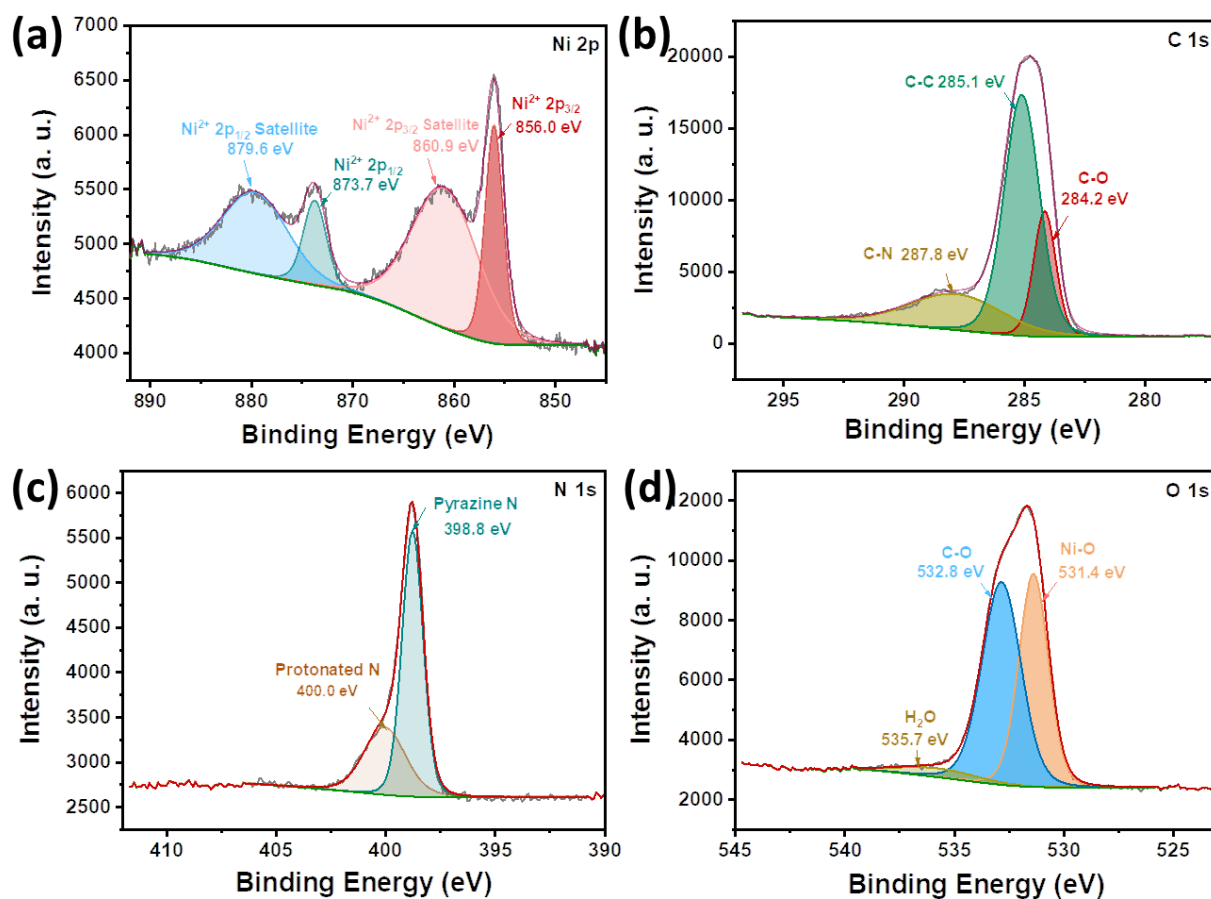


**Fig. S6** The XPS plots of each elements within the MOF(Ni). (a) Ni 2p; (b) C 1s; (c) N 1s; (d) O 1s.

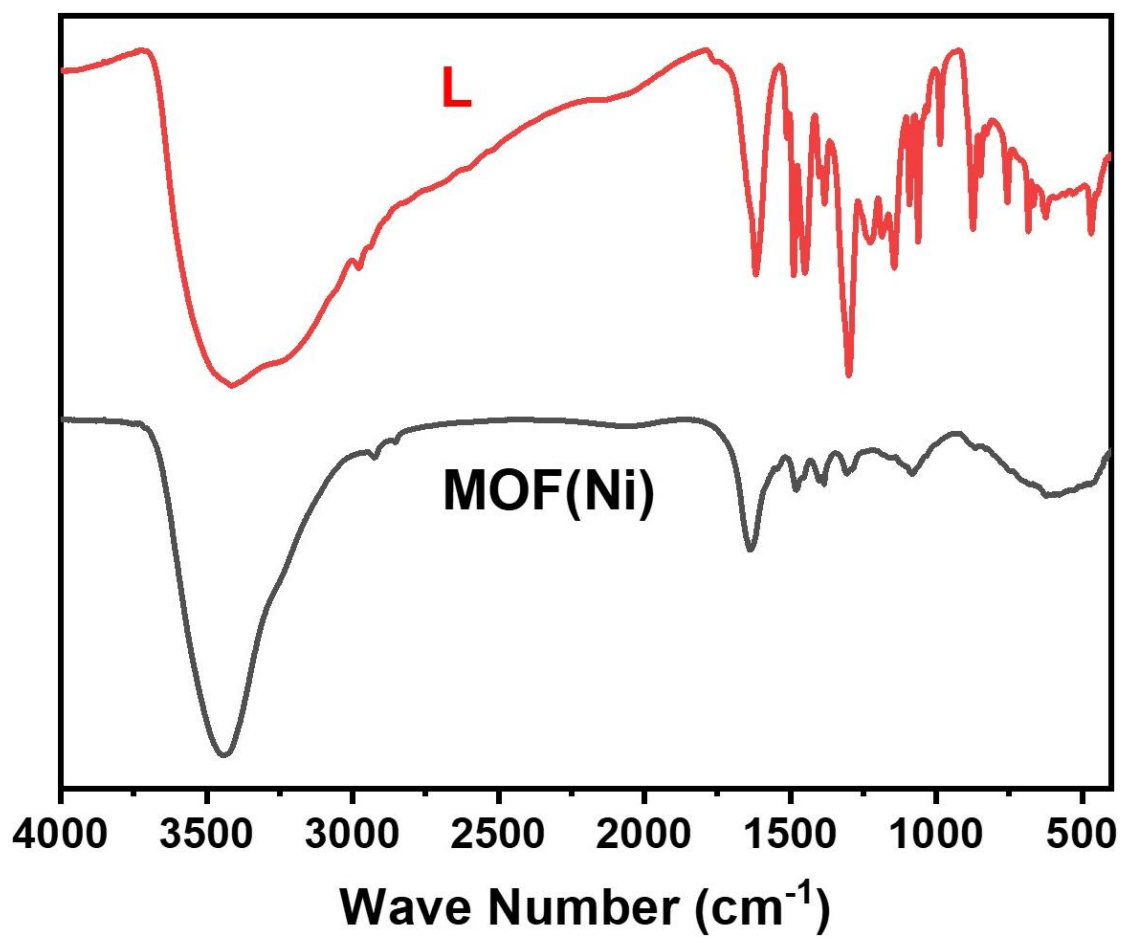


**Fig. S7** The FT-IR spectra of L and MOF(Ni).

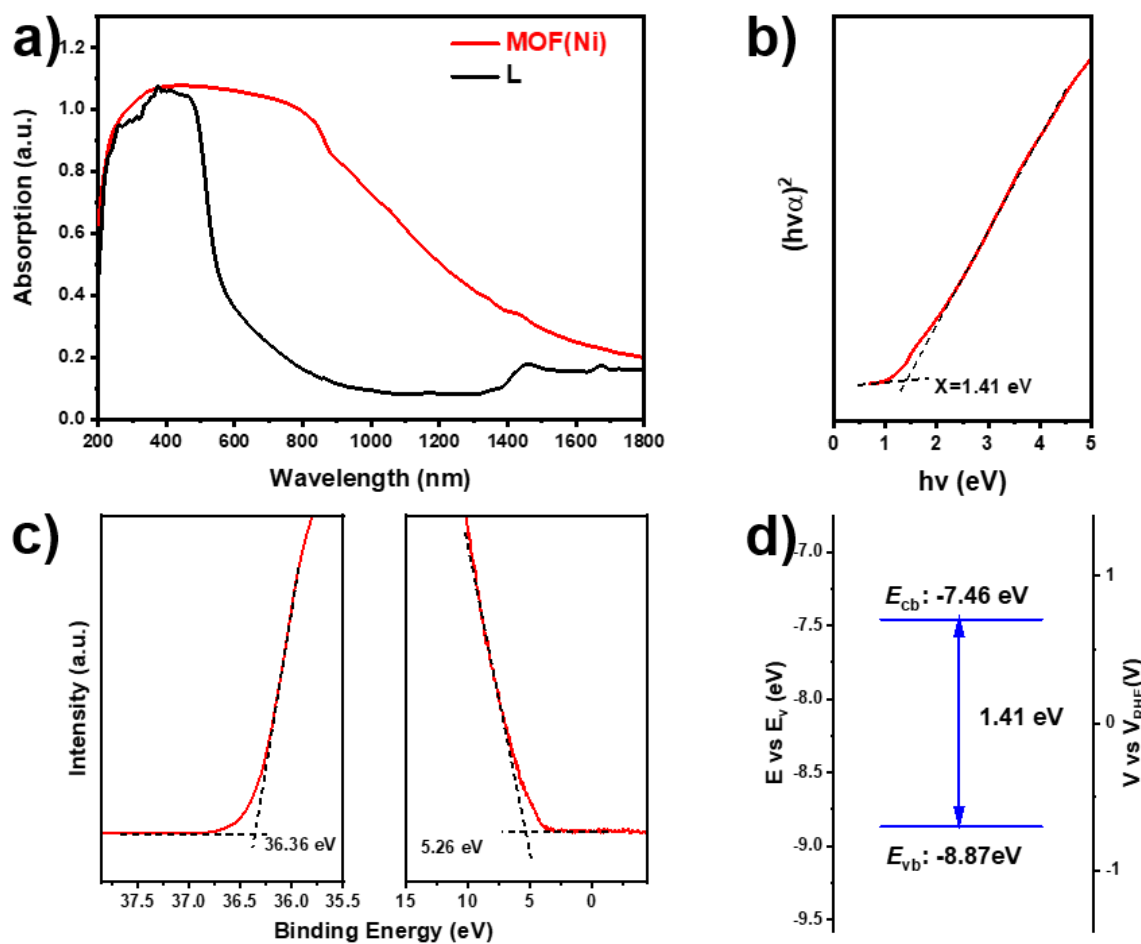
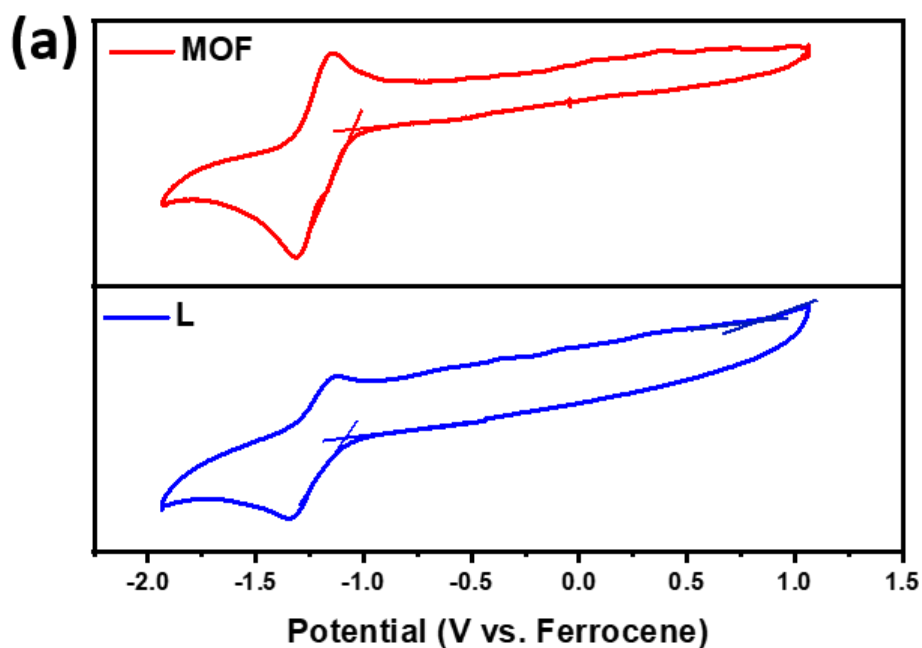


**Fig. S8** The UV-Vis-NIR and UPS spectra of MOF(Ni). (a) The UV-Vis-NIR spectra of **L** and MOF(Ni). (b)  $(h\nu\alpha)^2$  against  $h\nu$  curve of MOF(Ni). (c, d) UPS spectrum and  $E_{CB}$  and  $E_{VB}$  positions of MOF(Ni).



(b)

Entry	L (eV)	MOF(Ni) (eV)
Red	-1.09	-1.04
Ox	0.88	0.25
Eg	<b>1.97</b>	<b>1.29</b>
HOMO	-5.68	-5.05
LUMO	-3.71	-3.76

**Fig. S9** The CV curves and band energy of L and MOF(Ni) measured in CH<sub>3</sub>CN at a scan rate of 20 mV•s<sup>-1</sup>.

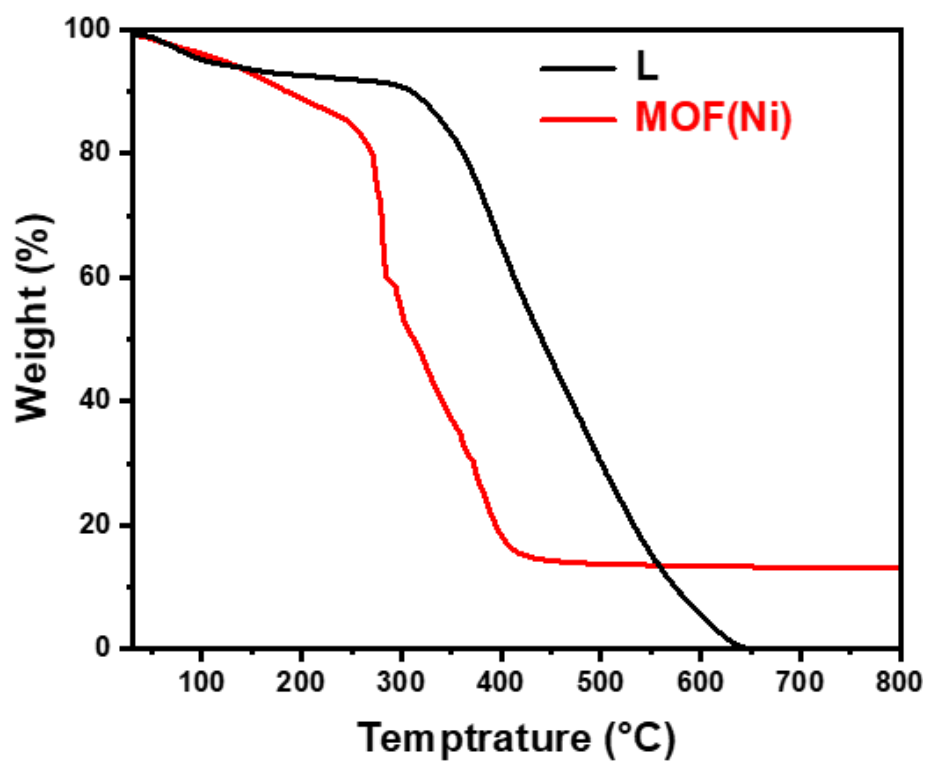


**Fig. S10** The TGA plots of L and MOF(Ni) under oxygen.

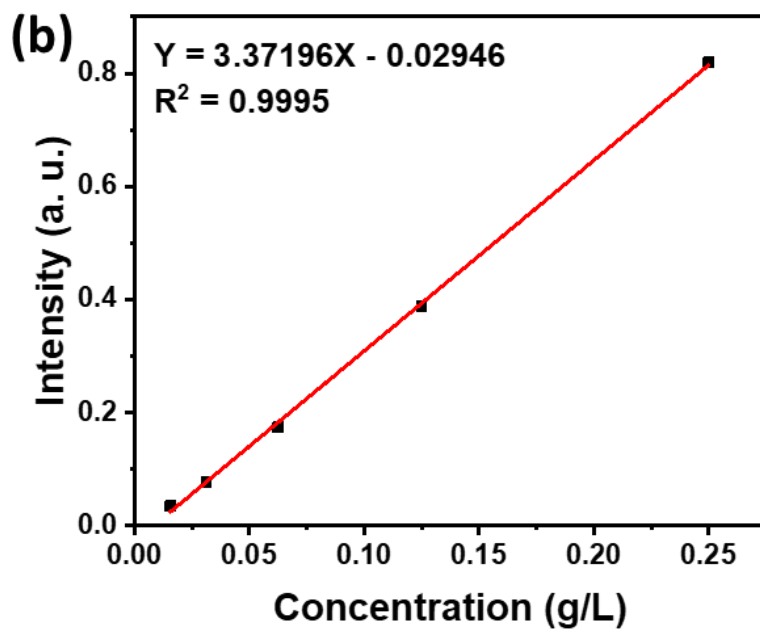
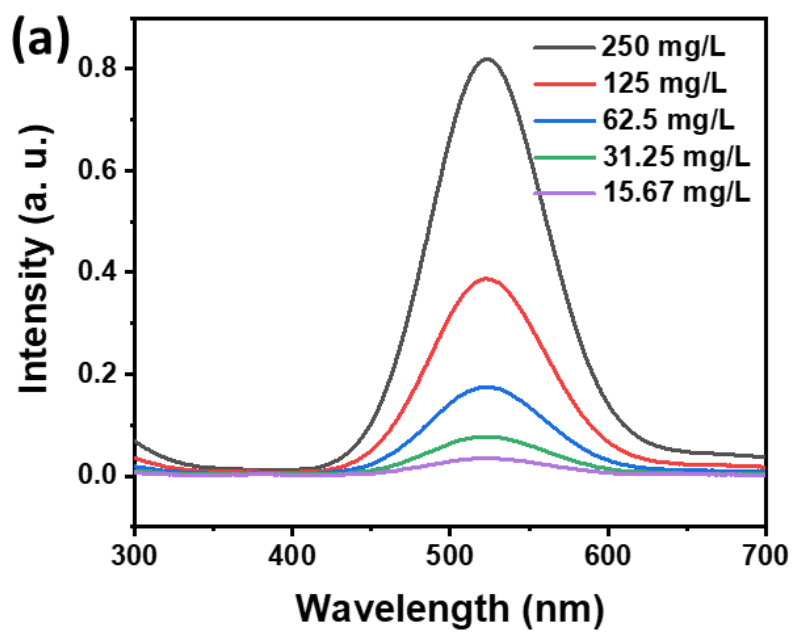


**Fig. S11** The standard curve of I<sub>2</sub> in cyclohexane.



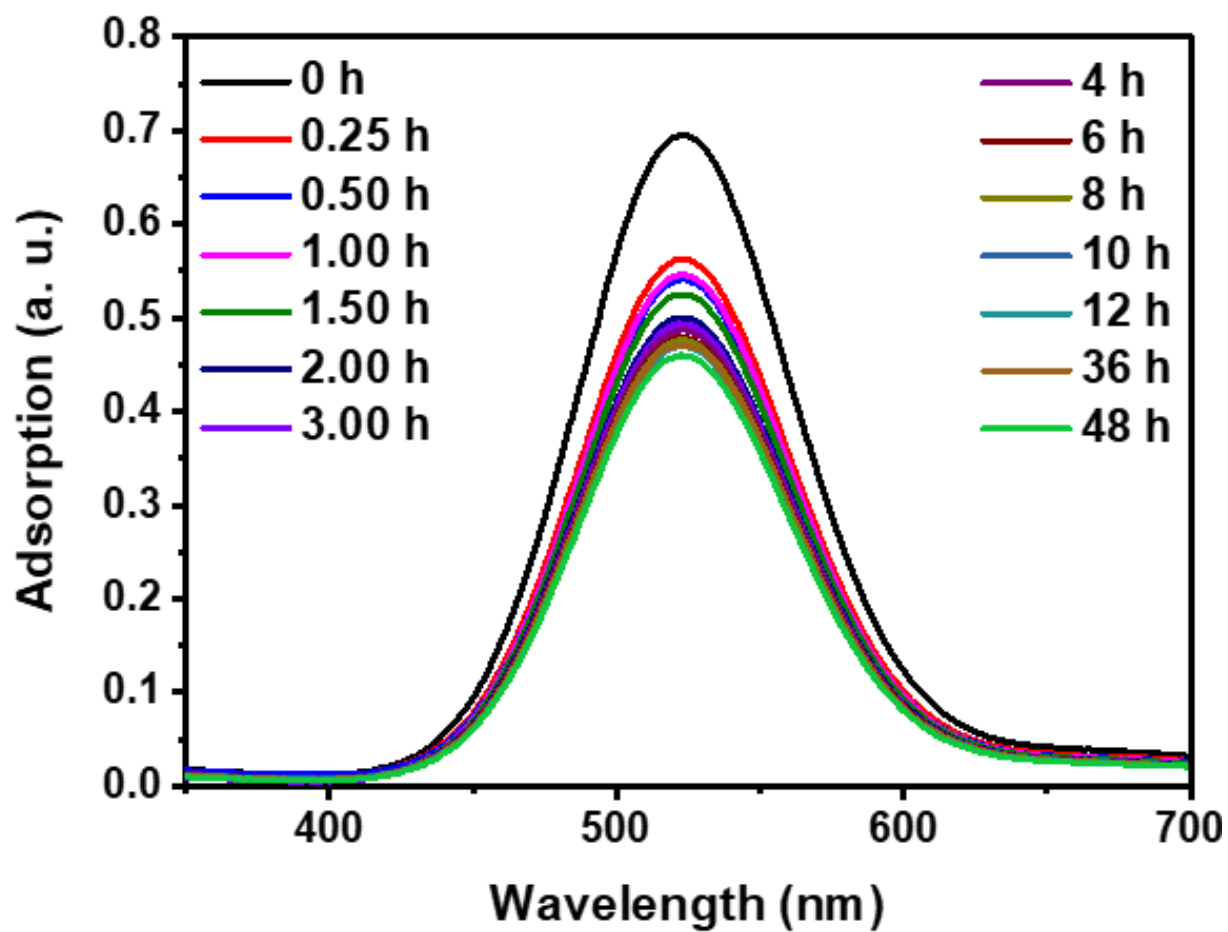


**Fig. S12** The UV-Vis curves of I<sub>2</sub> in supernatant after adsorption with MOF(Ni) for different times.

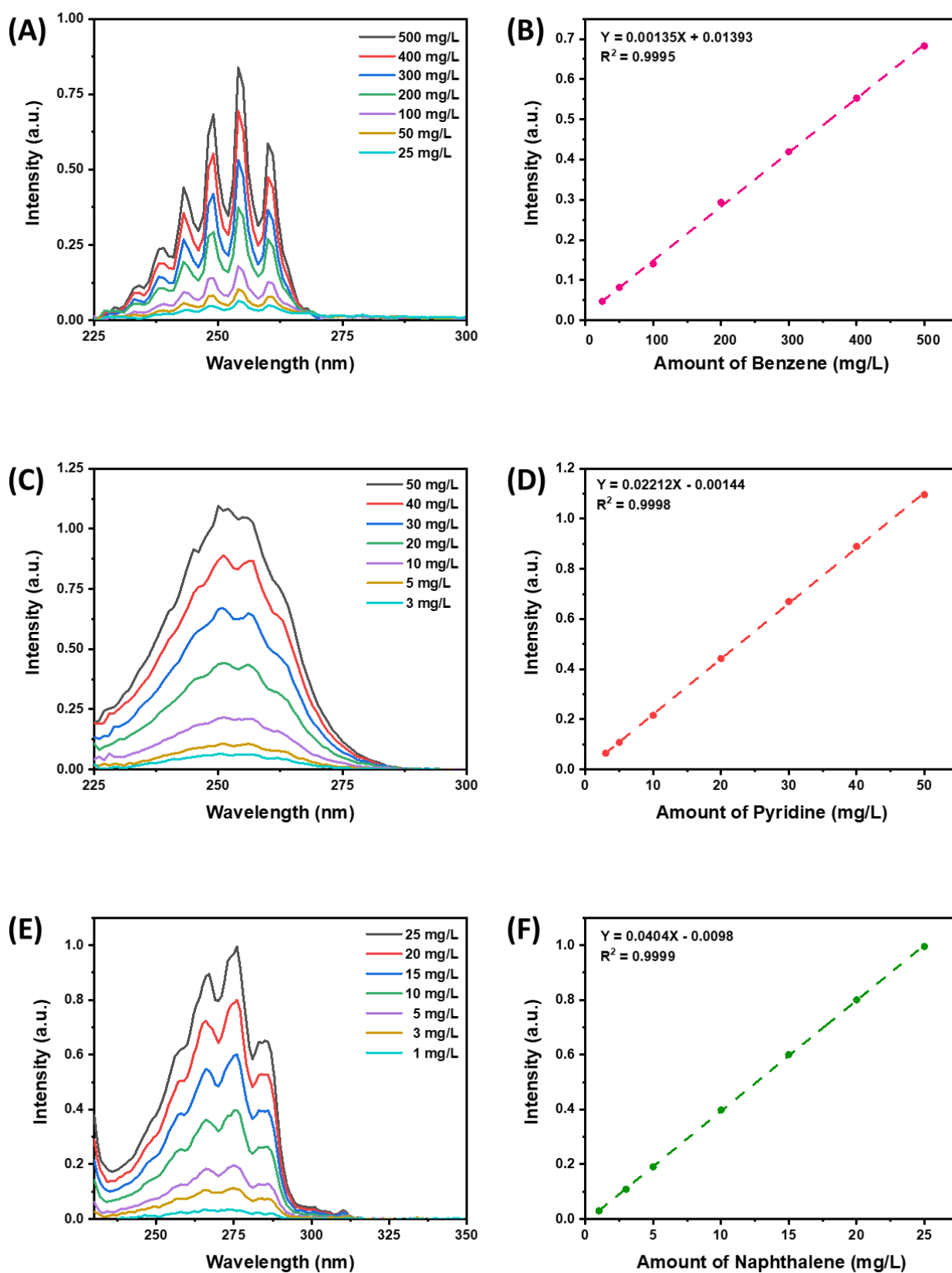


**Fig. S13** The standard curves of PAHs in  $\text{CH}_3\text{CN}$ . (A, B) for benzene at 249 nm, (C, D) for pyridine at 251 nm, (E, F) for naphthalene at 276 nm.

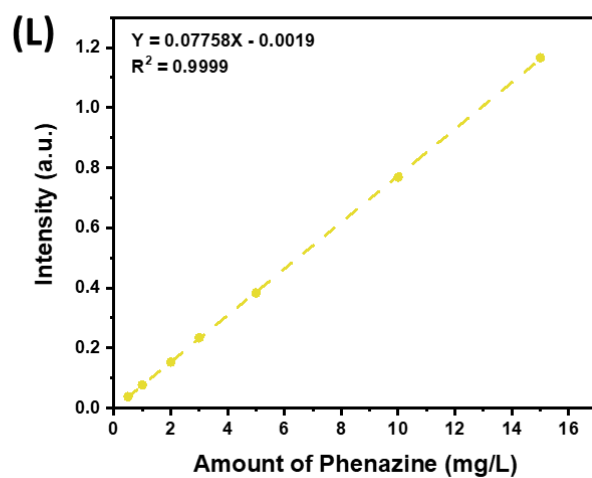
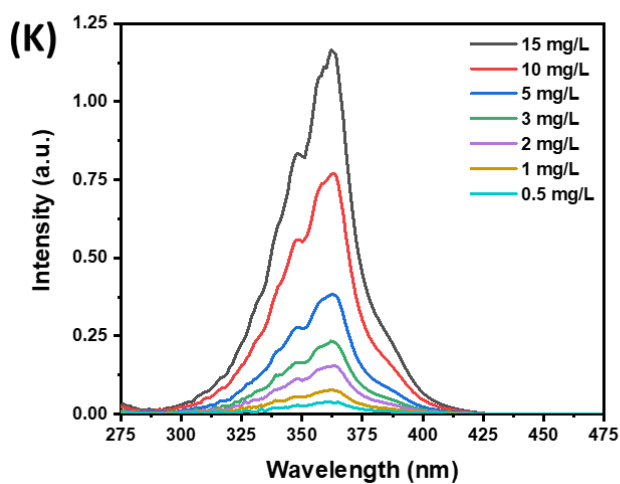
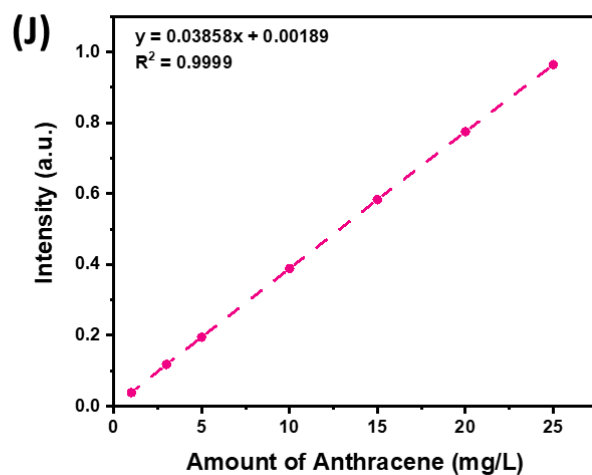
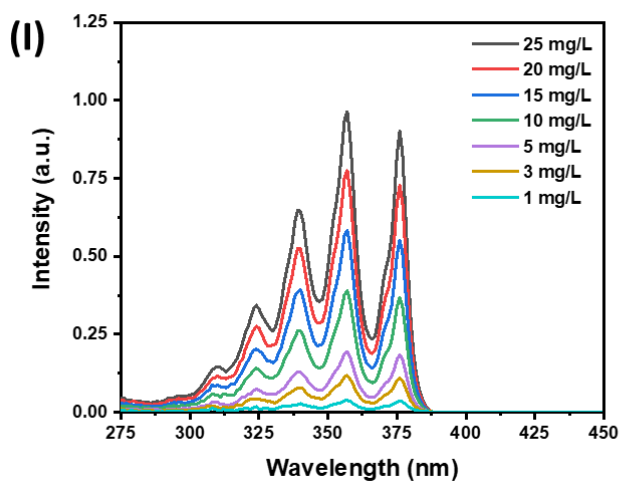
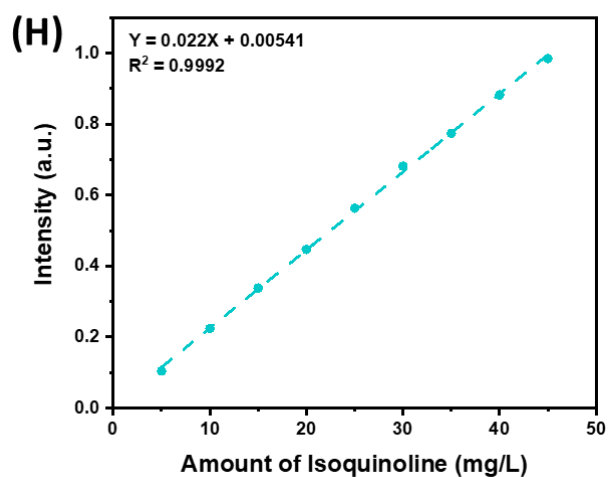
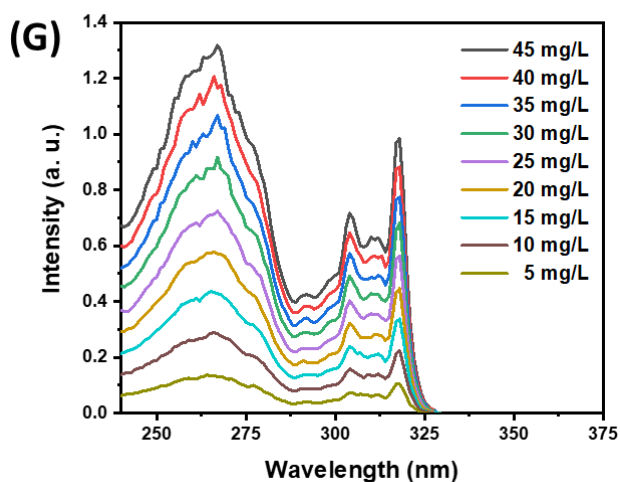


**Fig. S13** (continued) (G, H) for isoquinoline at 318 nm, (I, J) for anthracene at 357 nm, (K, L) for phenazine at 362 nm.

## Supporting References

- [1] Pan Y, Lin He, Youfu Wang. Ultrastable anion catechol frameworks (ACFs) of pentiptycene-based quad(catechol) through decavalent hydrogen bond. *ChemistrySelect*, **2022**, 7(1), e202103985.
- [2] Jingjuan Liu, Yi Zhou, Zhen Xie, Yang Li, Yunpeng Liu, Jie Sun, Yanhang Ma, Osamu Terasaki, Long Chen. Conjugated copper–catecholate framework electrodes for efficient energy storage. *Angewandte Chemie International Edition*, **2020**, 59(3), 1081-1086.
- [3] Hyuk-Jun Noh, Yoon-Kwang Im, Soo-Young Yu, Jeong-Min Seo, Javeed Mahmood, Taner Yildirim, Jong-Beom Baek. Vertical two-dimensional layered fused aromatic ladder structure. *Nature Communications*, **2020**, 11, 2021.